The Thesis Committee for Sangeetha Kumar
Certifies that this is the approved version of the following thesis:

A Simulation Framework to Characterize the Effect of Ventilation Control on Airborne Infectious Disease Transmission in Schools

APPROVED BY
SUPERVISING COMMITTEE:

Atila Novoselac, Supervisor

Richard Corsi, Co-Supervisor

A Simulation Framework to Characterize the Effect of Ventilation Control on Airborne Infectious Disease Transmission in Schools

by

Sangeetha Kumar

Thesis

Presented to the Faculty of the Graduate School of

The University of Texas at Austin

in Partial Fulfillment

of the Requirements

for the Degree of

Master of Science in Engineering

The University of Texas at Austin

May 2019

Acknowledgements

First and foremost, I would like to thank my two co-supervisors, Drs. Atila Novoselac and Richard Corsi for this opportunity to pursue graduate studies in engineering. Their substantial work and breadth in the fields of indoor air quality, building energy systems, and field studies in schools made this program a great fit for me. Their continued patience and support have lent to my growth as a researcher.

I'd like to acknowledge Leigh Lesnick, Michael Wade, Neil Crain, and Dori Eubank for their assistance in managing and conducting the Health High School PRIDE field study for which my thesis is based on. I'd also like to acknowledge Dr. Don Milton and Jacob Bueno de Mesquita of the University of Maryland at College Park School of Public Health for their assistance in understanding nuisances of airborne infectious disease modeling. A thank you to the consultants in the Department of Statistics and Data Science for answering my nuanced questions about developing distributions and running Monte Carlo simulations. Most importantly, I want to recognize my family and friends close and far for their undeniable support and encouragement these last two years.

I'd like to express my utmost gratitude to my sources of funding for graduate school and professional development activities:

- The University of Texas at Austin Cockrell School of Engineering for providing a first-year doctoral fellowship and the multi-year Thrust 2000 Burns/Fontaine Endowed Graduate Fellowship in Engineering.
- The University of Texas at Austin Office of Graduate Studies for providing a Professional Development Award to attend and present at the 2018 Indoor Air Conference in Philadelphia, PA.

- The Austin Professional Chapter of ASHRAE for providing funds to attend and present at the 2019 ASHRAE Winter Conference in Atlanta, GA.

The work described in this thesis was completed under Assistance Agreement 83563801-0 awarded by the United States Environmental Protection Agency (U.S. EPA) to the University of Texas at Austin. The thesis has not been formally reviewed by the U.S. EPA, and the views expressed in this thesis are solely those of the author. These views do not necessarily reflect those of the U.S. EPA, and the U.S. EPA does not endorse any products or commercial services mentioned in this thesis.

Abstract

A Simulation Framework to Characterize the Effect of Ventilation Control on Airborne Infectious Disease Transmission in Schools

Sangeetha Kumar, M.S.E.

The University of Texas at Austin, 2019

Co-Supervisors: Atila Novoselac & Richard Corsi

This study provides a detailed methodology for assessing the impact of ventilation control strategies on airborne infectious disease, specifically influenza, in schools. The probability of influenza infection in a classroom was approximated by the Rudnick and Milton (2003) model using inputs from a field campaign in Central Texas schools and reported influenza epidemiological data. The model is highly dependent on the quanta generation rate or the infectivity of an infector; therefore, a fractional removal term was developed to correct for filtration and depositional losses of the infectious quanta generated by the infector. Energy requirements for ventilation and associated outdoor air conditioning were estimated using air exchange rates and environmental quality conditions indoors (from the field study) and outdoors. To assess the variability in input parameters, Monte Carlo simulations were performed for different mechanical system types – split system and variable air volume (VAV) systems—and varying fractional removal terms. Assuming one infected student enters the school each day during the three-month period, the probability of infection ranges from 0.51% (9.5%) to 4.4% (6.3%). The corresponding number of secondary infections in a flu season range from ~400 to ~1100, which is in line with typical

influenza-like-illness absence rates of ~1% a day. The modeling framework considers five control strategies, increasing the ventilation rate by 20%, 40%, 60%, 80%, and 100% during the peak flu season of December to February. The largest benefit-to-cost ratios (BCR) due to reduced absenteeism were from increasing ventilation by 20% or increasing energy expenditures by $0.25/student for a single flu season. The greatest net benefits (NB) per student were from increasing ventilation by 100% (for some classrooms maintaining minimum ASHRAE standards for fresh air requirements) or increasing energy expenditures by $1.25/student for one flu season. Given the relatively low cost of energy for Central Texas, a hot and humid climate, increasing ventilation rates to adequate levels may prove beneficial for the well-being of students and staff. School systems may strongly benefit from this analysis to make better decisions on ventilating classrooms to reduce financial losses due to sickness related absences during the flu season.

Table of Contents

List of Tables

List of Figures

Introduction

Public school systems in the U.S. account for the second largest public enterprise in the country. By the time school-aged children—approximately over 50 million K-12 students—graduate from high school, they have spent upwards of 1.6 years inside school environments, the most time spent in an indoor environment other than their home [1,2]. Therefore, it is pertinent to characterize the school's environment and its impact on students. Increasing evidence demonstrates that a school's indoor environmental quality is known to have an effect on student performance, productivity, and health.

In the past two years, over 12 states have closed down schools due to widespread flu pandemics (absenteeism rates of greater than 20%) [3,4]. For states such as Texas and California, school absences are connected directly to state funding for public schools. Therefore, higher rates of influenza-like-illness absences can lead to funding losses for schools. The major pathways of influenza include direct contact, large droplet spray, and inhalation. Direct contact and large droplet spray transmission routes are widely recognized pathways for influenza transmission. Yet, given that children breathe larger volumes of air than adults [5] and increasing prevalence of school influenza outbreaks, perhaps the airborne transmission route is significant for schools.

Moser et al. (1979) completed one of the most notable epidemiological studies for potential proof of airborne transmission of influenza. The observational study in an aircraft found that an exposure time of 2 - 4.5 hours with a single infected passenger and mechanical ventilation turned off led to 72% of the crew and passengers with influenza-like illness and 91% of them with positive influenza tests [6]. These aerosol particles are small enough that they remain suspended in air and are not strongly influenced by gravitational setting losses. Influenza emission can occur through coughs, sneezes, and

exhaled breath where a large number of aerosols are released from the mouth. The airborne route of influenza can involve greater transport in air than direct contact or droplet nuclei.

Studies in the recent decade have further confirmed the existence of the airborne route of transmission specifically for influenza; however, the contribution of the airborne route of the flu is still being debated. Cowling et al. [7] estimated that the aerosol transmission route accounts for half of all transmission events. Atkinson & Wein [8] suspect aerosol transmission is the dominant mode of influenza transmission given the unlikelihood of close-up, unprotected droplet sprays. Nicas & Jones [9] found the inhalation route to be just as important as direct contact but stressed the lack of data on magnitude of infectivity in different regions of the body and transfer efficiencies for direct contact pathways. A review by Killingley & Tam [10] on routes of airborne influenza transmission found that all pathways are probable and conditions of the host, virus, and environment will dictate which pathway is most dominant.

Ventilation is the introduction of fresh air indoors for the purpose of diluting indoor air pollutants harmful to health. Ventilation can be provided naturally or through mechanical systems. Carbon Dioxide (CO_2) is often used as a proxy for estimating ventilation rates in buildings. The higher the CO_2 concentration, the lower the ventilation rate in the space and the more likely pollutants of human origin are able to persist at high levels indoors. A review of over 28 journal articles by Fisk et al. [11] found that all of the studies reviewed had classrooms with peak CO_2 concentrations greater than 1000 ppm. This indicates that most schools have inadequate ventilation rates as per ASHRAE Standard 62.1 Ventilation for Acceptable Air Quality [12]. While most of the school building stock in the U.S. is old, low ventilation rates in recently constructed or renovated buildings are still below minimum guidelines even for buildings certified as LEED or EnergyStar [13].

Lower ventilation in schools can exacerbate problems related to health and absenteeism. A review of 40 original studies by Li et al. [14] found sufficient and strong evidence to demonstrate a relationship between ventilation rates, movement of air, and airborne infectious disease (e.g., influenza, SARS, measles, tuberculosis) transmission. Inadequate ventilation rates have also been linked with increased student absences [15,16], and specifically illness related absences and increased visits to the school nurse [17–19]. Given the growing body of evidence of the airborne route of influenza transmission, engineering approaches such as ventilation control may be viable reduce flu cases.

Although many studies have characterized indoor air quality (IAQ) in schools, few have addressed the influence of increased ventilation on energy and retrofit expenditures. A study by Benne et al. [20] used building energy simulation tools to model school buildings. The study estimated that a mechanical ventilation rate of 6.3 L/s contributed 4.4% (16.4% of heating and 1.3% of cooling loads) to total building energy usage. A similar simulation study by Davangere et al. [21] found that increasing ventilation rates in Florida—a hot and humid climate—from 2.5 to 7.5 L/s would increase energy usage by 11.7-13.9% and heating, ventilation, and air conditioning (HVAC) operating costs by 17.1% - 19.8%. As evident by the former study, energy loads for ventilation are driven primarily by climate; seasonality changes in weather and extreme changes in climate will force buildings to expend more energy to heat and cool ventilation air. Additionally, significant energy usage is used to remove moisture from ventilation air in humid climates such as Florida.

The purpose of this paper is to characterize the effect of health-driven engineering control strategies in schools. We hypothesis that increased ventilation rates in mechanical systems can reduce the prevalence of airborne infectious disease and therefore reduce sickness-related absences in schools. To test this hypothesis, a Monte Carlo simulation

framework was developed to assess the effect of increased ventilation rates during the peak flu season on reducing the spread of influenza using a coupled airborne infectious disease-ventilation model. The model simulation uses indoor environmental and attendance data from a field study conducted in Central Texas high schools as well as flu vaccination data reported by the Center for Disease Control and Prevention (CDC) and in the literature. Estimates were calculated for probability of influenza infection in schools (and corresponding number of secondary infections) and ventilation energy requirements for hot and humid climates. The simulation framework considers multiple increased ventilation control strategies and a benefit-cost analysis was conducted to determine which is the most efficient and effective. The metrics developed in this assessment will be beneficial to school districts so they may make more informed decisions about influenza prevention.

Methodology and Relevant Background

The following section provides specifics details on the modeling framework used in this study as well as relevant background information on model inputs. The background information summarizes relevant findings and methodologies used in previous studies on epidemiological parameters for influenza. These discoveries will be introduced as they apply to modifications of existing models in this study. Additionally, this methodology section provides detailed analysis of school indoor environmental quality (IEQ) data from a field study in Central Texas schools.

FIELD STUDY

A two-year field campaign conducted in Central Texas high schools was used to characterize various indoor environmental quality parameters including but not limited to carbon dioxide, temperature, and relative humidity (RH). For a sampling period of four days each semester (Fall and Spring), two CO_2 sensors (Telaire 7001, Onset Corporation, Bourne, MA) were attached to a temperature and relative humidity sensor (HOBO U12, Onset Corporation, Bourne, MA) and placed in the supply ducts and classroom areas. Measurements were sampled at a 30 second frequency with a precision of ± 50 ppm (or 5%), ± 0.05^o F, and ± 0.05% RH respectively. During the 2015 – 2016 and 2016 – 2017 academic years, variations were captured in seven high schools, specifically 48 permanent classrooms and 10 portable classrooms. The data analyzed for this paper focuses solely on data in Spring 2016 and Spring 2017 for five high schools (40 permanent classrooms and 7 portable classrooms) because these time periods include the typical flu season months.

All of the schools sampled in this study use mechanical ventilation systems. The portable classrooms have wall-mounted air-conditioning (AC) units with On/Off catcalling driven by a thermostat (one AC unit per classroom). The permanent classrooms use

primarily multi-zone variable air volume (VAV) HVAC systems, with the exception of one school which used split HVAC systems (one split system per classroom). AC units in portable classrooms mix the air only in that specific classroom; whereas recirculation with VAV systems mix the air in multiple classrooms. The most common filters found in the air handling units (AHU) of the mechanical systems were rated MERV 7 and 8. In addition to the IEQ sampling, the school district provided attendance data based on classroom and class period for the 2015 – 2016 academic year as well as average daily attendance on a school level for the 2016 – 2017 and 2017 – 2018 academic school years.

AIRBORNE INFECTIOUS DISEASE MODELING

The simulations used in this study apply the Rudnick-Milton model [22] to estimate the probability that a susceptible person will be infected with influenza, P as:

$$P = \frac{D}{S} = 1 - \exp\left(\frac{-I\bar{f}qt}{n}\right) \quad (1)$$

Here, D is the number of disease cases in S susceptible individuals when in the same indoor space as I infectors. This probability is estimated as a Poisson distribution and is a function of the rebreathed fraction $\bar{f}$, the quanta generation rate q [quanta/hr], exposure time period t [hr], and the number of people in the space n. This equation is valid for steady state and non-steady state conditions and when the ventilation rate varies with time..

Rebreathed Fraction

The rebreathed fraction, $\bar{f}$, is a marker for exposure to exhaled breath from others in an indoor space and can be estimated based on a mass balance on CO_2 in an assumed well-mixed indoor space. Required parameters include the indoor CO_2 concentration (C), outdoor CO_2 concentration ($C_o \approx 400$ ppm), and exhaled CO_2 concentration ($C_a \approx 36{,}000$ ppm for all occupants). The rebreathed fraction does not require steady-state conditions, and it is representative of the CO_2 concentration during the entire exposure time period. It is calculatedas:

$$\overline{f} = \frac{(C - C_o)}{C_a} \quad (2)$$

If a space is properly ventilated by ASHRAE Standard 62.1 [12] ($C >$ 1,100 ppm), the corresponding rebreathed fraction would be greater than 0.019 or 1.9% of air in the space. An increase in rebreathed fraction corresponds to a larger probability of inhaling an infectious virus particle from an infector.

Quanta Generation Rate

The quanta generation rate, q, is defined as the generation rate of infectious quanta, or doses, by an infector. It is the average infected source strength of an individual carrying the infectious disease—considering both magnitude of infectivity and particle generation rates. Quanta generation rates are back-calculated based on epidemiological studies in planes and indoor spaces, using actual data on the number of infectors and susceptible people, and for influenza have been found to range from 15—515 quanta/hr [22–24]. A recent study by Yan et al. [25] quantified the infectious aerosol generation rate by collecting fine and coarse aerosol samples from patients with positive influenza tests. The sample population was told to breathe, talk, cough, and sneeze into a Gesundheit-II (G-II) human source bioaerosol sampler for a 30-min period. Coarse aerosol samples $> 0.5\ \mu m$ were collected on a filter and therefore lost potency so only fine aerosol samples were quantified for viruses using a focus-forming assay. The study found a geometric mean (GM) focus forming units (FFU) rate of 74/hr and geometric standard deviation (GSD) of 8.8/hr, with a minimum of 0 and maximum of 2200/hr. This large spread, and log-normal distribution, is consistent with the 'super-spreader' theory —certain infectors have a higher shedding rate than others [26,27].

However, in the case of Yan et al. (2018), one infectious aerosol dose does not necessarily equate to one infectious quanta. The data collected in Yan et al. (2018) does

not account for any control factors (sinks) of aerosols in the indoor space. In order to better estimate the infectious quanta generation rate in fine aerosols, different primary methods of removal of aerosols in the indoor environment need to be considered. Methods developed by Azimi & Stephens [28] built in this removal effect using existing data on aerosol deposition, filtration, and infectious aerosol size distributions from various studies. Their study uses the Wells-Riley model, and therefore they also included ventilation losses as well. However, the quanta generation rate applied in their study is back-calculated from epidemiological data; therefore, they are double-counting losses by adding explicit removal terms. For this study, a fractional loss term, σ_R, was developed to correct the quanta generation rate q found in Yan et al. (2018). This loss term accounts for particle deposition and filtration. Since the Rudnick-Milton model implicitly takes into consideration ventilation by way of the rebreathed fraction this ventilation loss term is neglected.

The fractional loss term can be estimated as $\sigma_R = (\lambda_{dep} + \lambda_{recirculation}\eta_{filter})^{-1}$. Where, λ_{dep} [1/hr] is the depositional loss coefficient, $\lambda_{recirculation}$ [1/hr] is the recirculation rate of air through the mechanical HVAC system, and η_{filter} is the removal efficiency of the filter in the mechanical system. Most of the studies considered in Azimi & Stephens (2013) include large fractions of influenza virus in coarse aerosols. However, based on results from Yan et al. (2018) and other recent studies, influenza virus is found at a larger fraction in fine aerosol measurements [26,29–31]. Therefore, following the same approach as Azimi & Stephens (2013), λ_{dep} and η_{filter} was estimated only for fine aerosols $< 0.5\ \mu m$ in three separate size bins: a) 0.3 – 1.0 μm, b) 1.0 – 3.0 μm, and c) 3.0 – 5 μm. Also, it was assumed that there was a uniform distribution in terms of infectious virus aerosol size since that was not studied in Yan et al. (2018); so, 33% of infectious virus was apportioned to each size bin. Removal efficiencies for a MERV 7 filter for the two smaller

size bins (a and b) were estimated by Stephens and Siegel (2012) and the large size bin was reported in ASHRAE Standard 52.2 [32,33]. These filter removal efficiencies are listed in Table 1. The total removal efficiency of the filter for aerosol particles < 5 μm can be estimated as the weighted-sum of the assumed particle size distribution and filter capture efficiency. The corresponding filter removal efficiency is $\eta_{filter} = 0.37$, which is in the range of values found in Azimi & Stephens (2013), 0.355 – 0.474, with a mean of 0.422 [28]. Using the geometric mean diameter of each size bin, deposition loss coefficients [1/hr] were estimated from Figure 3 in Riley et al. [34]. The geometric means and loss coefficient values of each size bin are listed in Table 1. The corresponding mean size-weighted average is $\lambda_{dep} = 0.71\ hr^{-1}$. The depositional loss coefficient in Azimi & Stephens [28] was $\lambda_{dep} = 1.7\ hr^{-1}$.

Table 1: Filter efficiency and deposition losses by aerosol size diameter

Size Bin [μm]	**Geometric Mean Diameter [μm]**	**Assumed Particle Size Distribution [%]**	**Filter Removal Efficiency [%]**	**Deposition Loss Coefficient [1/hr]**
0.3 – 1.0	0.55	33	17	0.1
1.0 – 3.0	1.7	33	46	0.45
3.0 – 5.0	3.9	33	50	1.6

Estimating the Reproductive Number

The reproductive number of influenza in a building, R_{AO},, is the number of secondary infections in susceptible occupants that arise when one infector is introduced into the space. The reproductive number is more accurate when adjusted for the number of susceptible people using reported flu data from the CDC including vaccination effectiveness, VE, and the proportion of the population vaccinated, P_{vac}. Therefore, Eq. 1 simplifies to:

$$D = R_{AO} = (n - I) \times (1 - VE \times P_{vac}) \times P \quad (3)$$

The CDC estimates influenza vaccination coverage using data from the National Immunization Survey-Flu (NIS-Flu) and the Behavioral Risk Factor Surveillance System (BRFSS) [35] by age group, state, and region of the United States. Analyzed data apportions patients into various sub-age groups, including high school aged children (13 – 17 years in age) for eight flu seasons between 2010 and 2018. In comparing the fraction of the population vaccinated in this age group in Texas and the U.S. overall, the fraction increases over time (between 2010 and 2018), 0.28 – 0.53 and 0.33 – 0.48 for each region respectively. A weighted sum approach of the number of patients surveyed and the probability of vaccination for each year was used to approximate the eight-year average. For Texas, the fraction of high-school aged students vaccinated was estimated to be $P_{vac} =$ 0.45 +/- 0.048, and for the U.S. it was $P_{vac} = 0.43$ +/- 0.014.

The CDC also reports data from epidemiological studies on vaccination effectiveness for each flu season. The adjusted vaccination effectiveness reported by each study for each flu season between 2006 and 2018 as well as the total number, n, patients screened for the study are shown in Figure 1. Adjusted vaccination effectiveness is approximated using a logistical regression model as $VE = 100 \times (1 - adj\ OR)$, where $adj\ OR$ is the adjusted odds ratio. Odds ratios compare the proportion of people vaccinated who tested positive for influenza with the proportion of people vaccinated who tested negative for influenza (test-negative controls) [36–43]; however, Jackson [28] compares the relative difference in influenza risk between vaccinated and unvaccinated participants. The odds ratios are later adjusted for various study parameters such as insurance status, age, sex, illness onset, and preexisting conditions. The average estimated adjusted VE

reported range from 0.19 to 0.60, but with large variance in estimation for earlier seasons (2006 to 2010) as evident by the large confidence intervals in Figure 1.

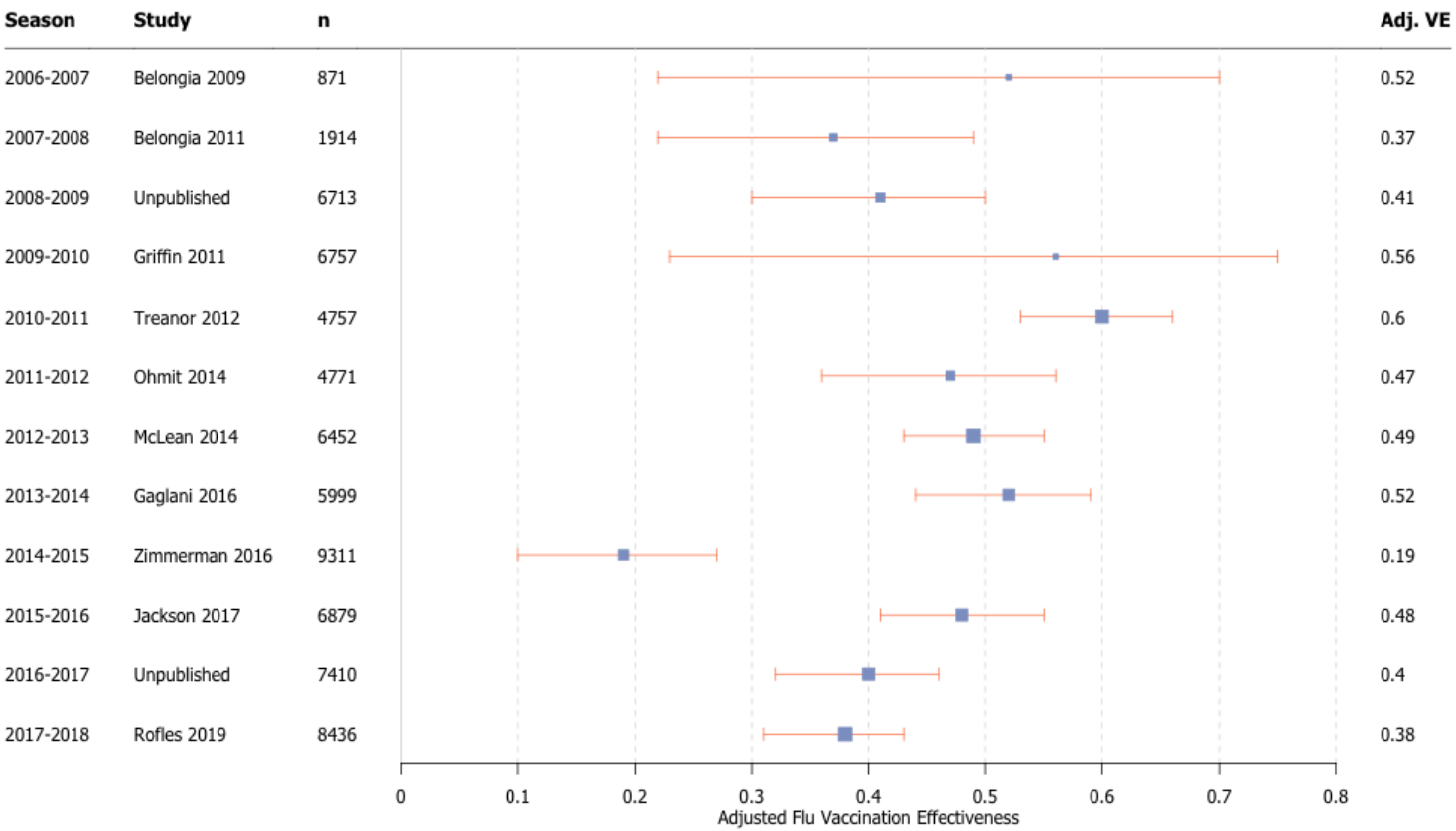

Figure 1. Adjusted flu vaccination effectiveness for 2006 – 2018 seasons as reported by the CDC

VENTILATION MODELING

Air exchange rates (ventilation rates) or the amount of outdoor air introduced indoors for dilution purposes was approximated using steady-state CO_2 measurements in the classrooms. Considering no other sources of CO_2 indoors other than humans and outdoors, the ventilation rate, λ, can be approximated as follows:

$$\lambda = \frac{nQ_bC_a}{V(C-C_o)} \quad (4)$$

The ventilation rate is a function of the number of people in the space n, a human's breathing rate Q_b [m^3/hr], the concentration of CO_2 on breath C_a, the concentration of CO_2 in the space C, the concentration of CO_2 outdoors C_o, and the volume of the space V [m^3]. The breathing rate for a human, average of a female sitting and a male sitting, from the California Air Resources Board (CARB) [44] is 8 L/min or 0.48 m^3/hr. Assuming a well-mixed space under steady state conditions, 45 min to 1 hr averages of CO_2 concentrations in classrooms were determined such that the coefficient of variation (CV) was less than 7%. The number of people in the space, n, was estimated using attendance data for a classroom on a class period basis. For periods in which attendance data were not present, particularly for Spring 2017, a mean value of attendance was used.

Energy required for ventilation can be thought of as the energy of bringing outdoor air indoors. Eq. 5 below estimates the energy requirements for ventilation.

$$Q_{vent} = \sum_{\tau=0}^{flu\ season} \frac{\dot{m}_{oa}(h_{oa}-h_{ia})}{COP} \quad (5)$$

Here, Q_{vent} is a function of the mass flow rate of outdoor air coming indoors, $\dot{m}_{oa} = \lambda\rho_{air}V$, where the density of air is $\rho_{air} = 1.2\ \left[\frac{kg}{m^3}\right]$, and the h_{ia} and h_{oa} are indoor and outdoor enthalpies of air [kJ/kg]. Assuming both heating and cooling use electrical energy, the efficiency of the system/coefficient of performance, $COP = 3$, was corrected for. The ventilation requirement is estimated for the entire modeled flu season where τ represents

each hour the system will be turned on during the flu season (number of days in the flu season × the number of hours in a school day).

Temperature and dew point temperatures were used to approximate values of indoor and outdoor enthalpies. Indoor enthalpy values were calculated using hourly averages of temperature and dew point temperature in each of the measured classrooms during occupied times. Outdoor enthalpy values were calculated using outdoor meteorological data from NOAA NCEI surface meteorological measurements [45] for Central Texas (WBAN 13904) for the 2017 to2018 time frame. The psychrometric chart in Figure 2 shows indoor and outdoor environmental parameters during occupied times of a typical peak flu season (December to February). The x-axis represents the measured temperatures in degrees Celsius and the y-axis represents the humidity ratio, or the air's ability to retain water, a function of dew point and temperature. The typical indoor set points are warmer during the winter time indicating that ventilation during the winter time will need to pre-heat outdoor air before introducing it indoors. Each of the greyed lines in the chart represents a relative humidity curve, the top most curve is a relative humidity of 100%. As demonstrated below, the outdoor values indicate high levels of humidity; therefore, schools will have an additional energy burden to dehumidify this air for ventilation.

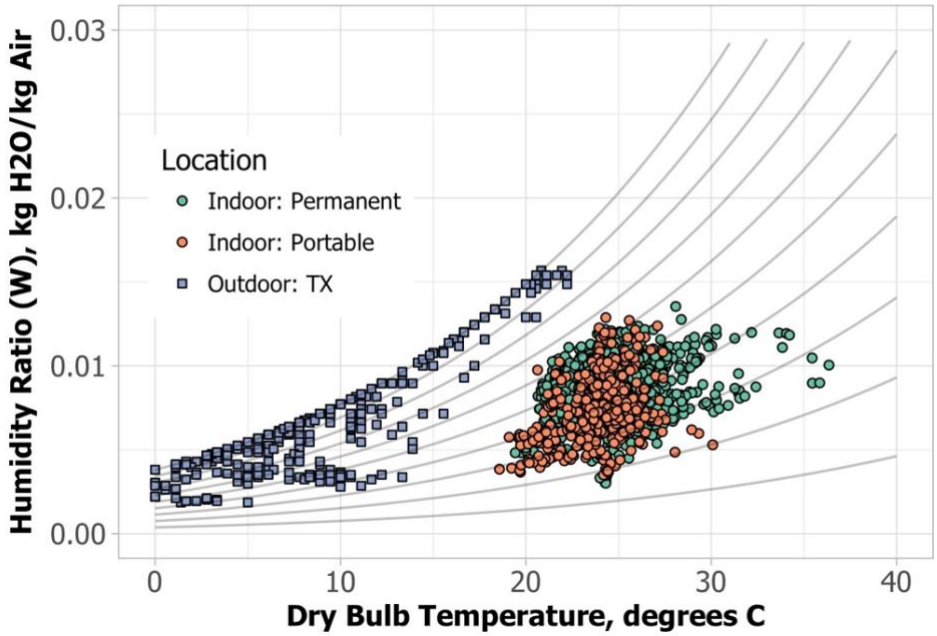

Figure 2. Psychrometric chart of indoor (portable and permanent) and outdoor temperatures and humidity ratios

SIMULATION FRAMEWORK

The framework for a Monte Carlo simulation to assess the cost effectiveness associated with increased ventilation during the peak flu season, December to February in schools is described in this section. Using a Lagrangian approach, the simulation follows a single infector, a student carrying the influenza virus, throughout their class schedule on a single day. The infector, with their own unique infectivity rate, attends seven one-hour occupied classes (neglecting the lunch period) in portable and permanent classrooms from 9:00 to 4:00 pm. Each of the classrooms has a unique number of students and associated rebreathed fraction. Based on a one-hour exposure time period, the probability of infection and the regeneration rate can be estimated using Eq. 1 and Eq. 3. For each day, the total number of disease cases is the sum across all class periods, and the probability of infection

is calculated for each class period. Any contact the infector may have with people outside of their classroom was ignored. The infector and anyone that has been infected (when the regeneration rate is greater than 1) is assumed to not come back to school the next day. This same exercise is completed for each of the 50 school days in the peak flu season, but with a new infector each time. The number of school days was estimated by a typical school academic calendar schedule excluding weekends and holidays. At the end of the season, the total number of flu cases is estimated across all days to approximate the fraction of students in a school that become ill by influenza. To ensure robustness of results, the simulation was iterated 10,000 times.

Model Assumptions and Inputs

Key assumptions for the simulation led to development of inputs based on constant values or probability distribution functions to capture variability and uncertainty in parameters. The following values use probability distribution functions from literature: quanta generation rate and vaccination effectiveness. The following values use probability distribution functions from the field data and are specific to classroom type: rebreathed fraction, air exchange rate, indoor enthalpy, and classroom attendance. To ensure non-negative parameter values for probability distribution functions, minimum and maximum values were chosen to bound selected estimates.

Since the primary HVAC system type in the schools was a multi-zone VAV system, multiple permanent classrooms were attached to the same air handling units. In the high schools that were measured, the number of classrooms to AHUs varied greatly from 4 to 35. For the simulation, a mean value of 16 classrooms were attached to a single AHU and all permanent classrooms attached to a single AHU create a giant room, resulting in air from one room being able to get to the other one. To take this into account, the number of students n was increased in Eq. 1 and 3 to include the number of students in the 15 other

classrooms. It is assumed that all of the other classrooms have roughly the mean attendance. Portable classrooms are considered to be self-contained, i.e., not connecting to other classrooms. The values for the quanta generation rate were pulled from a log-normal distribution of q with a GM of 74 quanta/hr and GSD of 8.8 quanta/hr and minimum and maximum values of 0 and 2200 quanta/hr from Yan et al. [25]. To correct for our removal term, σ_R, $\lambda_{recirculation}$ was estimated using data on set point air flows for permanent classrooms from the Energy Management team for the school district. Set points for supply airflow rates varied greatly from 3.5 – 16.8 hr^{-1}; yet, most of the values were around 7 hr^{-1}. Given that the outdoor air flow rate, λ has a geometric mean of 1.5 hr^{-1} in permanent classrooms (see Table 2), the recirculate rate is approximately $\lambda_{recirculation} = 5.5\ hr^{-1}$. Therefore, constant value of $\sigma_R = 0.36$ was used in the simulation.

The number of classrooms in the school was estimated using average class size and school size. In the school district that was sampled, four of the schools had populations between 2600 – 2800; with the exception of one school which has 3500 students (which was neglected in the calculation). Assuming classrooms are occupied at all times, each school has on average 113 classrooms (portable and permanent). All classrooms in the school are ventilated throughout the occupied hours; therefore, energy ventilation requirements are independent of infector's class locations. The air exchange rates and indoor enthalpies are the same across classroom type—portable and permanent. Rebreathed fractions for each of the classrooms were chosen such that they made sense with the ventilation rate and number of students in the classroom.

The model assumes that everyone has received the flu vaccine by December and that data estimates from Texas are representative of the U.S., so $P_{vac} = 0.45$ is the constant fraction of vaccinated students in the school. Rather than conducting a meta-analysis of the data represented in Figure **1**, each iteration of the Monte Carlo simulation chooses a flu

season from the provided data and randomly selects for a vaccine effectiveness, VE. It was assumed that the distributions reported in each of the papers follow a normal distribution, and the minimum and maximum values are the lower and upper bound confidence intervals. The effect of previous history of vaccination or built up immunity to the influenza virus as well as strain of influenza was neglected.

The following parameters from the school study were analyzed and developed into probability distributions for use in the simulation: rebreathed fraction, enthalpy, attendance, and air exchange rates (ventilation rates). Histograms of the analyzed data, separated by classroom type, are presented in Figure 3. Rebreathed fractions and indoor enthalpies were estimated using 1-hr averages of CO_2 concentrations, temperature, and relative humidity in rooms during occupied hours. Rebreathed fraction data were removed if there were indicators of no occupancy including lack of attendance data, static CO_2 concentrations throughout the school day, or low CO_2 concentrations. A minimum hourly average threshold of 500 ppm CO_2 was adopted. Indoor enthalpies and ventilation rates were computed as aforementioned earlier in the methodology, and no data was removed in the analysis of the indoor enthalpies.

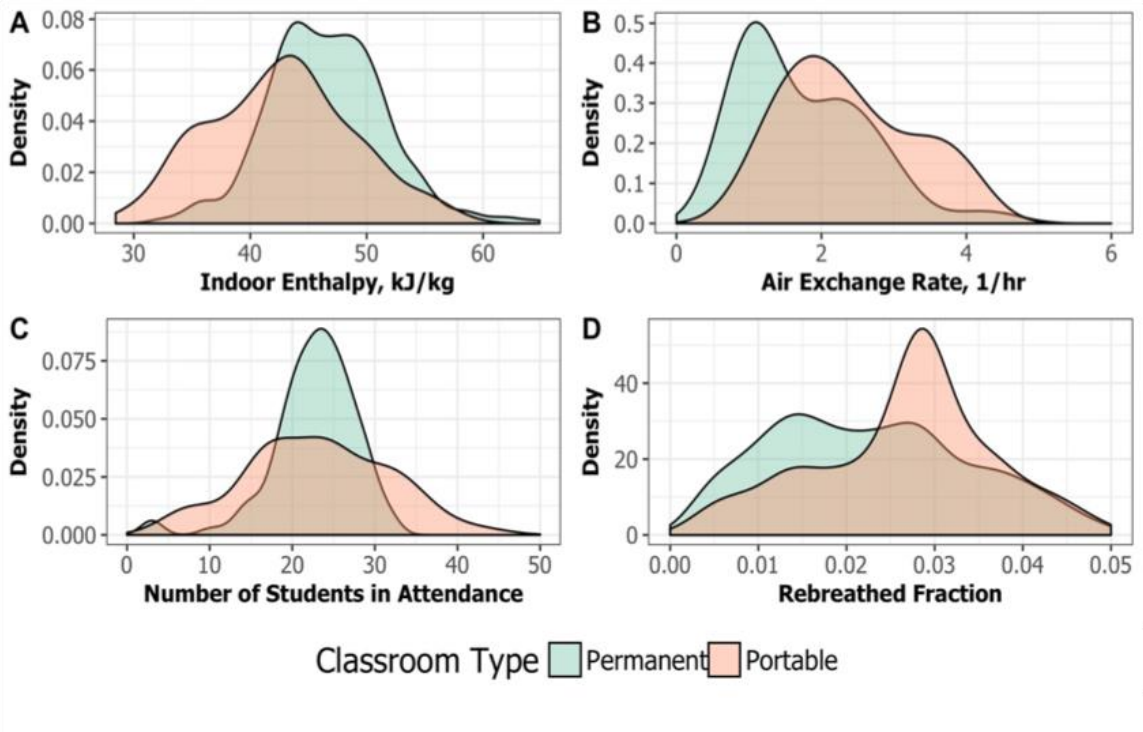

Figure 3. Probability density functions of school environment input parameters

In order to develop distributions of the various input parameters, the experimental data was fit to normal distributions using Kolmogrov - Smirnov (K-S) equality of distribution tests. The mean, standard deviation, minimum, and maximum of each distribution that will be sampled in the Monte Carlo Simulation by classroom type are provided in Table 2. Indoor enthalpy, classroom attendance, and rebreathed fractions in portable classrooms all follow normal distributions. In permanent classrooms, indoor enthalpy and classroom attendance also follow normal distributions. As demonstrated in Figure 3 above, the rebreathed fractions varied greatly amongst classrooms and class periods. In order to best model this large variability, a multimodal log normal distribution with three peaks was adopted. The total distribution can be thought of a sum of three different distributions, where the apportion of each distribution to the whole is denoted by

λ_1, λ_2, and λ_3. The geometric mean and standard deviation of the different peaks, or modes, are listed in Table 2.

Air exchange rates follow log normal distributions with geometric means and geometric standard deviations. Comparing these calculated rates with the required ventilation requirements using room-specific maximum enrollment and classroom volumes, 100% and 62% of portable and permanent classrooms respectively are under-ventilated as per ASHRAE Standard 62.1 [12]. Average values for portable and permanent classrooms, 5.0 (1.3) L/s-person and 4.5 (1.6) L/s-person, are consistent with ventilation rates in schools found in literature which range from 2.9 – 8.4 L/s-person on average. The ventilation rates found are most consistent with findings of 4.4 L/s-person in [46] , 5.4 (4.3) L/s-person in [47], and 4.2 (2.3) L/s-person in [48] for classrooms with mechanical ventilation systems. The low ventilation rates can be attributed to HVAC systems being shut off during unoccupied periods, fresh air dampers turned off to save energy, and outdoor air vents obstructed by tape. The portable classrooms may have artificially higher ventilation rates due to their 'leaky' structure. Using Google Earth Satellite Imagery and school populations, 20% of a school's classrooms were estimated to be portable classrooms and 80% were permanent. Classroom volumes are constant across classroom types and are based on averages of classrooms that were sampled.

Table 2: Distributions of field data used in the Monte Carlo Simulation

Parameter	Portable Classrooms			Permanent Classrooms		
	Sample Size	**Mean (SD)**	**Min, Max**	**Sample Size**	**Mean (SD)**	**Min, Max**
Indoor Enthalpy, h_{ia} [kJ/kg]	372	42.7 (6.2)	28.4, 58.9	1034	46.6 (5.0)	31.8, 64.9
Rebreathed Fraction, $\bar{f}$	290	0.0290 (0.0126)	0.0028, 0.0583	914	[1] 0.0046 (1.3) [2] 0.0157 (1.3) [3] 0.0324 (1.5)[a]	0.0028, 0.0583
Number of Students, n[c]	81	23 (9)	5, 44	241	23 (5)	3, 32
Air exchange rate, λ [1/hr]	35	2.2 (1.5)[a]	1.0, 6.4	58	1.5 (1.6)[a]	0.6, 4.5
Fraction of classrooms	0.2			0.8		
Volume, V [m^3]	159			254		

[a] Due to large variability in this parameter, sampled data was fit using a multi-modal log normal distribution with three separate peaks. Values listed here are geometric means and geometric standard deviations of each peak. The lambda values associated with each peak are as follows $\lambda_1 = 0.07$, $\lambda_2 = 0.47$, $\lambda_3 = 0.46$

[b] Attendance data is only based on reported values from Spring 2016

[c] The values described represent geometric mean (GM) and geometric standard deviation (GSD) as the distributions were found to be log-normally distributed.

Ventilation Control Strategies

We are interested in computing the benefits and costs associated with different ventilation strategies and how they influence the probability of airborne infectious disease transmission. The ventilation strategies are defined and driven by the air exchange rate, λ, more specifically the difference in air exchange rate between the current modeled scenario and the control strategy, $\Delta\lambda$. The effect of increasing ventilation during occupied times was investigated using five different ventilation control strategies: 1.2λ, 1.4λ, 1.6λ, 1.8λ, and 2λ. To understand the effect of increased ventilation and probability of airborne infectious

disease transmission, the rebreathed fraction $\overline{f}_{\Delta\lambda}$ is back-calculated by manipulating Eq. 4 into:

$$\overline{f}_{\Delta\lambda} = \frac{nQ_b}{V\Delta\lambda.} \tag{6}$$

This a rough estimate of what the rebreathed fraction should be in a class period given that the mechanical HVAC systems are providing the proper ventilation rates. From this new rebreathed fraction, the corresponding probability of infection, ΔP, and new regeneration rate (number of disease cases), ΔR_{AO} can be estimated.

To understand the cost effectiveness of the control strategies, consider two different metrics: the benefit to cost ratio (BCR) and the net benefits (NB). The benefit of a specific ventilation strategy is the amount of money ($) a school saves from reduced absenteeism. For this study we did not quantify benefits associated with reduced costs to parents of staying home to care for an ill child or reduced medical bills for families. The cost of the ventilation strategy is the extra cost of energy associated with increased ventilation during occupied times of the school day. The goal is to find optimal control strategies that result in a BCR > 1 and NB > 0 for one school in one flu season. BCR and NB are represented below in Eq. 7 and Eq. 8.

$$BCR = \frac{Benefits}{Costs} = \frac{\Delta R_{AO} \times \$/abs \times abs}{\Delta Q_{vent} \times E_{cost}} \tag{7}$$

$$NB = (\Delta R_{AO} \times \$/abs \times abs) - (\Delta Q_{vent} \times E_{cost}) \tag{8}$$

The CDC recommends that students with flu-like symptoms stay home for at least a 24-hour period. Each student who contracted the flu was absent for abs = 1 day, and on average the school district loses $\$/abs = \$45$ of revenue from the state per student for each absent day based on values in Central Texas school districts. The cost associated with ventilating the space is the unit cost of electricity specifically for Texas or $E_{cost} = \$0.08/kWh$ (from estimates published by the U.S. Energy Information Administration (EIA) [49]).

Results & Discussion

The largest sources of uncertainty in estimating probability of influenza infection in classrooms are the fractional loss term σ_R and type of HVAC system (i.e. system per classrooms or VAV that mixes air in-between multiple classrooms). To characterize a range of probabilities, six different scenarios were considered– three different fractional loss terms and two different types of HVAC systems. To account for a larger fraction of infectious virus in coarse aerosols, the fractional loss term was estimated as $\sigma_R = 0.25$, using $\lambda_{dep} = 1.7\ hr^{-1}$ and $\eta_{filter} = 0.422$ from Azimi & Stephens [12]. A more conservative estimate of $\sigma_R = 0.50$ was also considered to account for more of the influenza virus in the fine aerosol particle size range. A split HVAC system (1 AHU to 1 Classroom) was compared to a Multizone VAV System (1 AHU to 16 Classrooms) where the number of susceptible students increases proportionally to classroom/AHU ratio.

Simulation results for these combinations are provided in Figure 4. Each subplot A to F represents a unique combination of HVAC system and σ_R. The larger plot is a density histogram of the probability of infection in classrooms with an infector. The smaller plots are cumulative probability distribution functions (CDFs) of the number of secondary illnesses or the reproductive number for the school given the simulated probabilities. The dotted grey line on each of the spots provides a reference to the 50th percentile (or median) value.

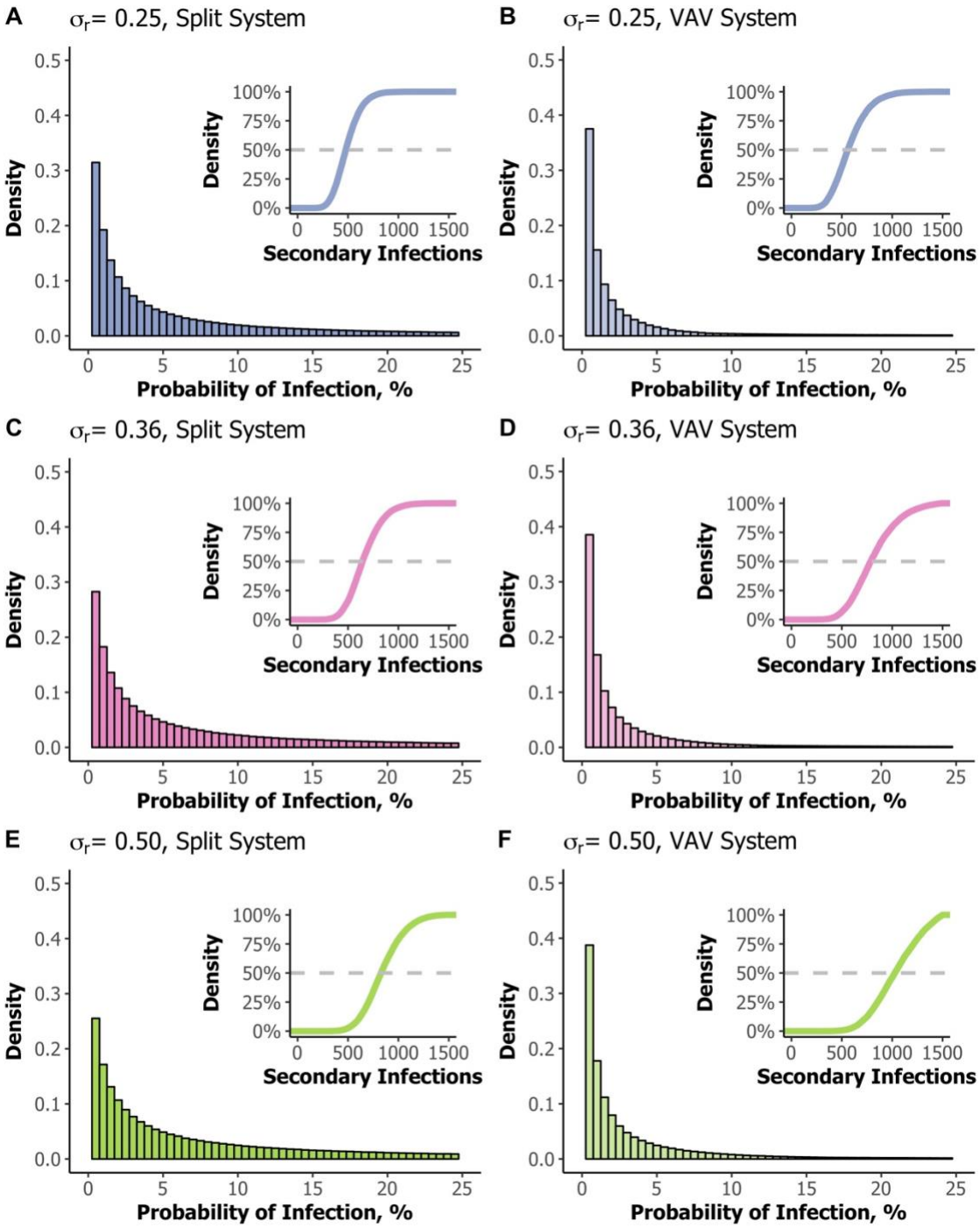

Figure 4. Probability of infection in a classroom and number of secondary illnesses (reproductive number of influenza) for a school across an entire flu season

Results for probability of infection in classrooms with an infector follow a log-normal distribution with long-tails and GSDs. This is indicative of the nature of the quanta generation rate and its strong effect on influenza risk. Despite large variability in rebreathed fraction for permanent classrooms (which are more prevalent in schools) probability of flu seems predominantly dependent on the infectivity rate of the infector. These results further validate the super-spreader theory that different infectors have different rates of infectivity [26,27,31].

As demonstrated in subplots A, C, and E of Figure 4, the GM (GSD) probability of influenza for split systems for each increasing value of σ_R is 2.2% (6.7)%, 3.2% (6.5%), and 4.4% (6.3%). These risk values subsequently lead to a 50% percentile of ~ 480, ~ 640, and ~ 830 secondary infections across the entire school (with 2700 students) for one flu season. Likewise, for subplots B, D, and F of Figure 4 demonstrate that the probability of influenza in VAV systems for varying σ_R values are respectively 0.26% (9.7%), 0.37% (9.6%), and 0.51% (9.5%) leading to ~ 560, ~ 790, and ~ 1080 secondary infections. Increasing values of σ_R, less particle losses due to deposition and filtration, lead to higher probabilities of infection. VAV systems have lower influenza risks than split systems because of the increased number of people in the room; however, this assumption increases the number of susceptible students (due to the air mixing in-between 16 classrooms by air recirculation) resulting in a larger number of secondary infections.

The type of HVAC system did not influence energy requirements for ventilation. Considering the 'business as usual' scenario of no increased ventilation, the energy requirement per student to ventilate an average sized school for the flu season follows a lognormal distribution with a GM (GSD) of 15.9 (1.5) kWh/student or $1.30/student. As aforementioned, ventilation energy requirements are strongly influenced by climate. To demonstrate this fact and further assess the developed framework, the Bay Area in

California (specifically, San Francisco) was simulated—a marine, temperate climate—using 2017 – 2018 meteorological data from NOAA's NCEI meteorological database [45] for met station WBAN 23234. Figure 6 below is an update of Figure 2 including San Francisco's reported temperatures and calculated humidity ratio. The pink boxes in the plot represent the outdoor values in Central Texas; whereas, the blue boxes represent that of San Francisco. As evident by the smaller spread of data, The Bay Area's climate is more temperate and less humid during the winter months.

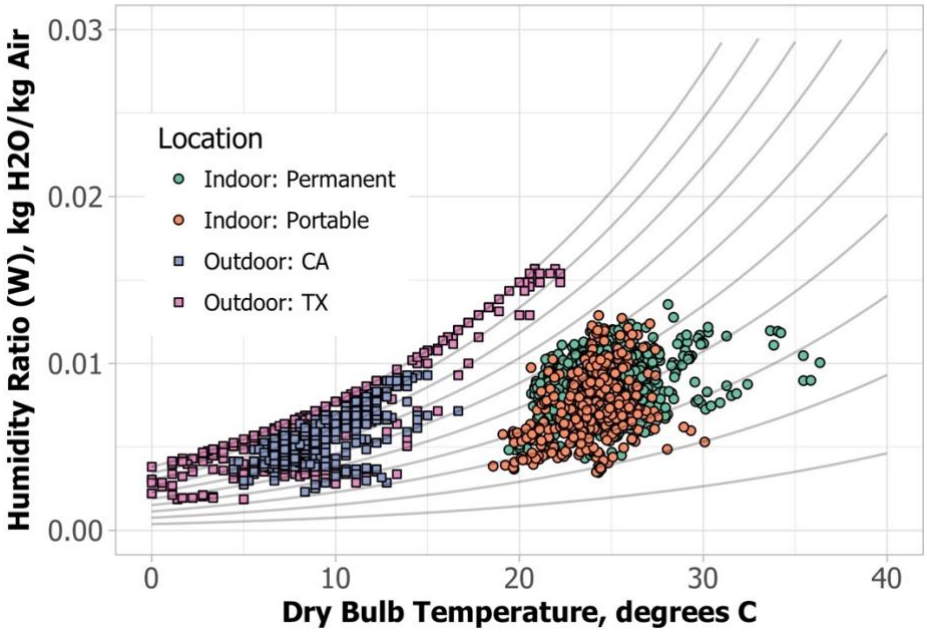

Figure 5. Psychrometric chart of indoor (portable and permanent) and outdoor temperatures and humidity ratios in Central Texas and San Francisco, California

Using a unit of electricity cost of $E_{cost} = \$0.15/kWh$ from U.S. EIA [49] for California, the energy requirement per student to ventilate an average sized school for San Francisco has a GM (GSD) of 13.5 (1.5) kWh/student or $2.00/student. While the ventilation related energy loads were consistently higher for Central Texas than Bay Area

even in the winter months because of the need to decrease the humidity of outdoor air coming indoors; the elevated unit cost of electricity in California leads to overall higher costs per student.

In this study, we looked at the effect of five different ventilation control strategies: 1.2λ, 1.4λ, 1.6λ, 1.8λ, and 2λ. The corresponding increase in energy usage kWh/student and increase in energy costs $/student by location and strategy are visualized in Figure 6 and Figure 7, respectively. For each simulated ventilation control strategy, the increase in ventilation energy per student for the integrated flu season is consistently higher in Central Texas vs. San Francisco. A 20% increase in air exchange rates corresponds to an increase in 3.1 kWh/student and 2.7 kWh/student for Texas and California during the flu season. A 100% increase in the ventilation rate at schools results in an extra energy expenditure of 15.6 kWh/student and 13.3 kWh/student. However, increased costs don't follow a similar pattern as evident in Figure 7. In San Francisco, increasing the ventilation by 80% and 100% is more expensive than increasing the ventilation by 100% in Texas. A 20% increase in air exchange rates corresponds to an increased cost of $0.25/student and $0.40/student for Texas and California, respectively. A 100% increase in the ventilation results in a $1.25/student and $2.00/student increase in energy related expenses over the entire flu season.

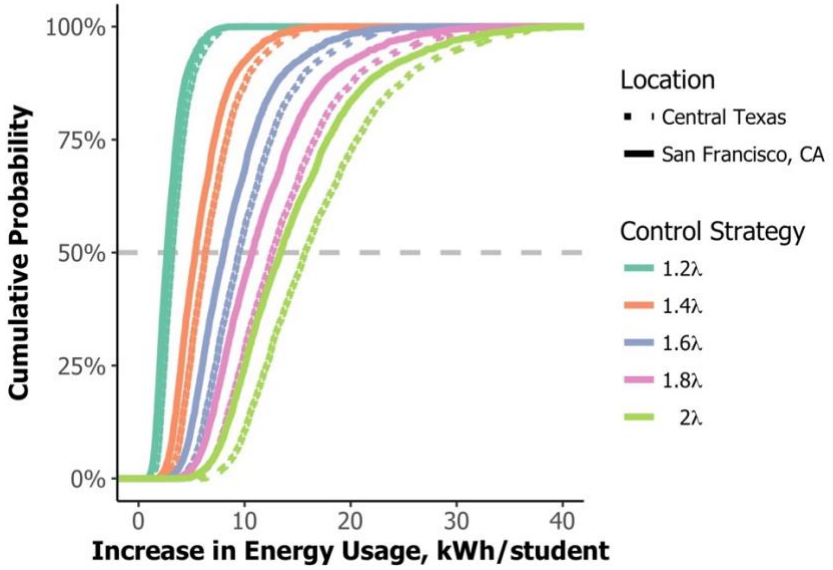

Figure 6. Comparison of increased ventilation energy requirements (kWh/student) between Central Texas and San Francisco, California for entire flu season

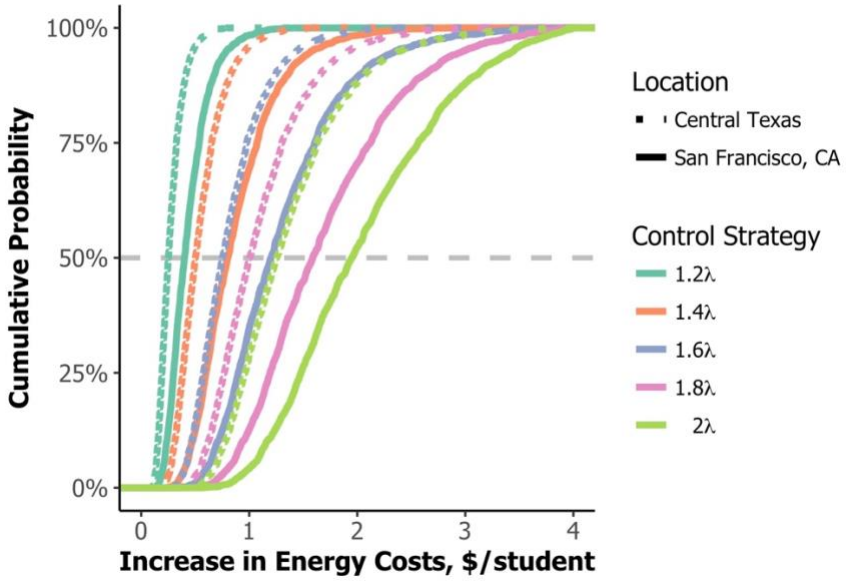

Figure 7. Comparison of increased ventilation costs ($/student) between Central Texas and San Francisco, California for entire flu season

Coupling the results from the ventilation energy and airborne infectious disease modeling, we can assess which of the ventilation strategies is the most effective and cost-efficient. For each control strategy, the BCR to the school and NB per student were calculated. Optimal solutions will have NB > 0 and an incremental BCR > 1. To characterize the variability in the benefit cost analysis, two extreme scenarios were modeled (lowest and highest number of secondary infections): (a) σ_R = 0.26 with a split system and (b) σ_R = 0.50 with a VAV system. The cumulative distribution functions of benefit-to-cost ratios and net benefits for each control strategy are demonstrated in Figure 8 and Figure 9, respectively. Using the 50th percentile value as a benchmark for the simulation results, all control strategies are optimal. The largest BCR was for 1.2λ (increasing ventilation by 20%), (a) BCR = 10 for the split system and (b) BCR = 25 for the VAV system. The greatest NB per student for both system types was 2λ (increasing ventilation by 100%): (a) \$3.50/student and (b) \$10/student. To reiterate, the high BCR and NB values for VAV systems are representative of the increased 'exposed' population of students in near-by connected classrooms.

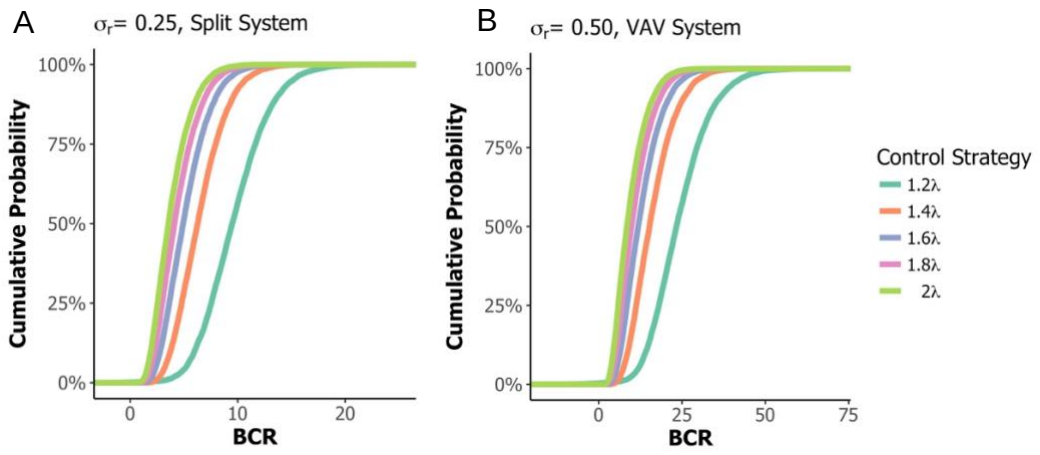

Figure 8. Benefit to Cost Ratio (BCR) to the school for a flu season by fraction removal loss and HVAC system type

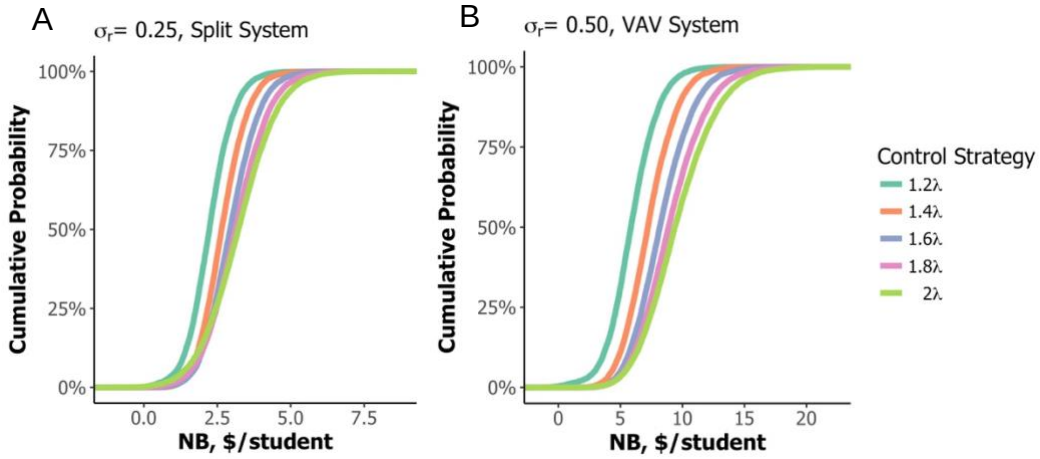

Figure 9. Net Benefits (NB) per student to school for entire flu season by fraction removal loss and HVAC system type

COMPARISONS TO EXISTING STUDIES AND RELEVANT DATA

A similar study was conducted in California by Mendell et al. (2013) to quantify the effect of increased ventilation rates on reduced illness-related absences. To compare our results, the cost of an absence as $\$/abs$ = \$29 for California was adopted from Mendell et al. [17]. Using aforementioned ventilation energy estimates from San Francisco, CA, the

corresponding BCR and NB values were compared to those reported in the Mendell et al. (2013) the study. Similar to results in Texas, the largest BCR was for 1.2λ or BCR = 4 in a split system and BCR = 10 for the VAV system. The greatest NB per student for a split system resulted from a 20% increase in ventilation rates or NB = $1.20/student and a 100% increase in ventilation rates for a VAV system where NB = $5/student. Mendell et al. (2013) considered two increased ventilation strategies, 1.8λ and 2.4λ. Only considering benefits of increased state revenues to schools, the study's BCRs and NBs are approximately 8.3 or $4.70/student and 9.0 or $9.40/student [17]. Our results fall within the order of magnitude found in this study, indicating that different methodologies lead to similar outcomes—increased ventilation is cost-beneficial to schools to reduce illness-related absenteeism.

Class period attendance for classrooms were collected for 2015 to 2016, and monthly school level attendance was provided from 2016 to 2018. A common metric school districts use to assess attendance is average daily attendance (ADA) or the percentage of students in the school present that given day. Classroom level attendance data in sampled spaces indicate a lower number of absences (~1%) across all classroom types in fall 2015 (256 absences, 95.6% ADA) in comparison to spring 2016 (347, 96.8% ADA). Measurements in the spring semesters were taken during the winter months, and therefore attendance is representative of the actual peak flu season. Similarly, in school-wide data by month, there is an increased rate of absenteeism ~1 – 2 % during the peak flu season above the baseline absenteeism rate in late summer and earlyfsall. These findings further validate that perhaps in the spring semester students in these specific classrooms were more likely to be absent.

The school and classroom level attendance in the field study did not code the reason for absence; therefore, we considered publicly available data from California, New

Hampshire, and New Jersey to find comparable values. The Mendell et al. [17] field study measured an illness related absence rate in California elementary schools during the winter months of 2.32 – 2.75%. Both the New Hampshire Department of Health and Human Services [50] and The State of New Jersey Department of Health [51] report influenza-like-illness (ILI) absence rates in schools for all counties throughout the year. Only reports from Week 48 to Week 8 (reflective of December – February time frame) were considered. The most frequent ILI rate was 0.1 – 0.9% in New Hampshire and of 0 – 1.5% in New Jersey. Both states peaked in absenteeism during the peak of the flu season (late January to early February) where ILI rates reached up to 5% in certain counties but more commonly 1.5 – 3%. These influenza specific absenteeism rates match increased absence rates in Central Texas during winter months. Note, none of these values include estimates on multiple-day absences. Therefore, it is reasonable to assume that in comparison to non-flu months there is a 0 – 3% increase in average daily absenteeism in winter months due to flu-like illness.

STUDY LIMITATIONS

As noted in previous sections, one of the largest sources of uncertainty is fractional removal term, σ_R, for the quanta generation rate. The simulation framework developed in this thesis assumes that the quanta generation rate, $q = 74\ quanta/hr$, from Yan et al. (2018) does not implicitly account for any particle removal by deposition and filtration in the bioaerosol sampler. The human bioaerosol sampler used in their study, the Gesundheit II collects fine aerosol samples through a slit impactor with an 85% capture efficiency [52]. This high capture efficiency of fine aerosols proves that particle losses in the sampling process can be negligible.

The model described also only accounts for the inhalation pathway. While more evidence in literature has increased confidence in the airborne transmission route of influenza, the contribution of the airborne pathway to total secondary infections is still unknown. Therefore, estimations of probability and number of secondary infections should potentially be higher. Only considering the airborne route and utilizing ventilation as a control strategy perhaps magnifies the true effect of the control strategy. Additionally, school aged students, especially in high school, are highly variable. There is a lack of understanding on how students come in contact with each other throughout the day. Addressing these gaps in social networks can lead to understanding how influenza is passed from one student to another.

One of the largest limitations of this model is accurately assessing the fraction of students that are absent due to the flu. As aforementioned in the simulation framework methodology, the number of secondary infections was calculated as the summation across the entire flu season for each classroom using Eq. 3. Assuming an average school size of 2700 students, the modeled ILI absence rate ranged between 0.3 – 0.9%. Although the number of secondary infections in all modeled scenarios seem high, they are reflective of actual average school flu absence data, 0 – 3% absent per day. The number of infectors in the flu season is one of the strongest drivers of this number. This parameter has a linear relationship with the reproductive number. So, assuming an infected student comes into school during the peak flu season every other day, this would reduce the number of secondary illnesses by half. For days with higher rates of influenza-like illness, there would be more infectors entering the school or students with multiple-day absences due to severity of symptoms.

The applied model neglects the inactivity of airborne pathogens as they are suspended in air. Deposition is a large removal term for coarse aerosols; however, for fine

aerosols other than ventilation, inactivity is a large removal mechanism. Studies have found a positive linear correlation between inactivation rates of infective aerosol virus and relative humidity in the space [53,54]. Yang & Marr [55] found that high humidity levels indoors (RH ~ 90%), not typically found during the drier, winter months, have the ability to increase inactivity by 28% [55]. However, these high humidity levels may be uncomfortable to occupants. The typical relative humidity values found indoors in our field study ranged greatly from 15 – 64% across both portable and permanent classrooms. We did not account for how the relative humidity in the space could reduce the amount of infectious viral aerosols.

Another large assumption in this framework is how to consider movement of infectious aerosol virus in a multi-zone VAV mechanical system where multiple classrooms share the same AHU. The modeled assumed all of the classrooms would turn into a 'well-mixed' box; however, that might not be the case when recirculation rates are not high. For more precise results, the model can be updated to consider multi-zone modeling and computational fluid dynamic models. These methods, however, might be computational intensive and result in similar results. To & Chao [24] suggest implementing numerical models that utilize computational fluid dynamics (CFD) methods to approximate dispersion and deposition in spaces. Noakes & Sleigh [56] developed a stochastic inter-zonal model to assess how proximity to the infector influences probability risk.

For the ventilation control strategies chosen, increasing ventilation rates to ~ 1.6λ and ~ 2λ for permanent and portable classrooms is equivalent to providing the minimum requirements for fresh air as per ASHRAE Standard 62.1. It is practical to increase these ventilation rates in existing mechanical HVAC systems, so increased HVAC equipment costs to handle higher ventilation rates were not considered. Fisk et al. [11] estimated increasing ventilation rates to meet or exceed current standards would amount to less than

0.1% of education spending. According to the National Center for Education Statistics, as of 2014 the U.S. on average spends ~ $12,300 per student on primary and secondary education [57]. Extrapolating our estimates for ventilation costs per student to the entire school year, this amounts to almost $8/student for ~ 2λ, or 0.1% of educational spending. Indirect costs such as decreased costs of caregiver to the family and substitute teacher costs to the school for absent teachers were not considered.

This study also did not consider the effect of improved filtration on reducing probability of influenza infection. Based on particle removal efficiency data by Stephens & Siegel [32], an increase in MERV rating increases the loss deposition rate for aerosol in the fine aerosol size bin with the exception of the 0.3 – 0.5 μm range. Improved filtration to a higher MERV ratings imposes an additional energy cost due to the pressure drop across the filter. In a prospective study in an office setting, Azimi & Stephens [28] found that improved filtration to MERV 13 – 16 was more cost effective at reducing influenza risk than increased outdoor ventilation rates. However, the effect of the filter is highly dependent on the recirculation rate through the mechanical HVAC system. Increasing recirculation rates would in turn reduce the outdoor ventilation rates; therefore, schools would need to make informed decisions on which control strategy is the most cost effective and cost efficient.

Conclusion

A previous field study found that both portable and permanent classrooms sampled in Central Texas are slightly under-ventilated [58]. Expanding on this study, we investigated if increased ventilation rates can reduce the spread of influenza in the airborne pathway and if they are a cost-effective control strategy to schools. Through conducting an airborne infectious disease and ventilation model-based Monte Carlo simulation of a school throughout the flu season, the following are key takeaways:

- The probability of influenza infection in any given classroom in a school is heavily dependent on the infectivity, the quanta generation rate q, of the infected student.
- The regeneration rate, or reproductive number of influenzas, is highly dependent on type of mechanical ventilation system (based on modeling assumptions) and number of infected students that enter the school each day. Simulated number of flu cases for a school year during the peak flu season align with values found for influenza-like-illness daily absenteeism of 0.1 – 3% depending on the number of infected students.
- Increasing ventilation rates to 2λ is equivalent to actually providing the minimum requirements of ventilation for many of the classrooms. It is also the most cost effective and efficient at reducing number of secondary illnesses due to airborne routes of influenza.
- Energy requirements for ventilation vary greatly by climatic region; however, total cost of ventilation is driven also by local cost of electricity and natural gas.

Further work in progressing this simulation framework should focus on characterization of the influenza's virus aerosol size distribution and dynamics in the air,

impacts of improved filtration, modeling multi-zone mechanical ventilation systems, and assessments of other indirect costs and benefits due to lower sickness. Given the low cost of energy, the large cost associated with student absences, and the optimality of all modeled control strategies, it is worth it for schools to provide adequate fresh air rates.

References

[1] N.E. Klepeis, W.C. Nelson, W.R. Ott, J.P. Robinson, A.M. Tsang, P. Switzer, J. V Behar, C. Hern, W.H. Engelmann, The National Human Activity Pattern Survey (NHAPS): a resource for assessing exposure to environmental pollutants, (2001).

[2] E. Eitland, L. Klingensmith, P. MacNaughton, J.C. Laurent, J. Spengler, B. Ari;, J.G. Allen, Schools for Health: Foundations for Student Success How School Buildings Influence Student Health, Thinking and Performance, 2018. www.ForHealth.org.

[3] S. Scutti, As flu season takes a turn for the worse, some schools close in at least 12 states, CNN. (2019). https://www.cnn.com/2019/01/25/health/flu-update-cdc/index.html.

[4] J. Christensen, Flu Slams Schools, Shuttering Some, CNN. (2018). https://www.cnn.com/2018/01/26/health/flu-schools-shut-down/index.html.

[5] I. Annesi-Maesano, N. Baiz, S. Banerjee, P. Rudnai, S. Rive, the S. Group, Indoor Air Quality and Sources in Schools and Related Health Effects, J. Toxicol. Environ. Heal. Part B. 16 (2013) 491–550. doi:10.1080/10937404.2013.853609.

[6] M.R. Moser, T.R. Bender, H.S. Margolis, G.R. Noble, A.P. Kendal, D.G. Ritter, An outbreak of influenza aboard a commercial airliner., Am. J. Epidemiol. 110 (1979) 1–6.

[7] B.J. Cowling, D.K.M. Ip, V.J. Fang, P. Suntarattiwong, S.J. Olsen, J. Levy, T.M. Uyeki, G.M. Leung, J.S.M. Peiris, T. Chotpitayasunondh, H. Nishiura, J.M. Simmerman, Aerosol transmission is an important mode of influenza A virus spread, Nat. Commun. 4 (2013) 1935–1936. doi:10.1038/ncomms2922.

[8] M.P. Atkinson, L.M. Wein, Quantifying the routes of transmission for pandemic influenza, Bull. Math. Biol. 70 (2008) 820–867. doi:10.1007/s11538-007-9281-2.

[9] M. Nicas, R.M. Jones, Relative contributions of four exposure pathways to influenza infection risk, Risk Anal. 29 (2009) 1292–1303. doi:10.1111/j.1539-6924.2009.01253.x.

[10] B. Killingley, J. Nguyen-Van-Tam, Routes of influenza transmission, Influenza Other Respi. Viruses. 7 (2013) 42–51. doi:10.1111/irv.12080.

[11] W.J. Fisk, The ventilation problem in schools: Literature review, Indoor Air. (2017) 1039–1051. doi:10.1111/ina.12403.

[12] ASHRAE, ANSI/ASHRAE Standard 62.1-2013. Ventilation for Acceptable Indoor

Air Quality, 2013.

[13] S. Batterman, F.C. Su, A. Wald, F. Watkins, C. Godwin, G. Thun, Ventilation rates in recently constructed U.S. school classrooms, Indoor Air. 27 (2017) 880–890. doi:10.1111/ina.12384.

[14] Y. Li, G. Leung, J. Tang, X. Yang, C. Chao, J. Lin, J. Lu, P. Nielsen, J. Niu, H. Qian, A. Sleigh, H.-J.J. Su, J. Sundell, T. Wong, P. Yuen, Review Article Role of ventilation in airborne transmission of infectious agents in the built environment – a multidisciplinary systematic review, Indoor Air. 17 (2007) 2–18. doi:10.1111/j.1600-0668.2006.00445.x.

[15] D. Shendell, R. Prill, W. Fisk, M. Apte, D. Blake, D. Faulkner, Associations between classroom CO2 concentrations and student attendance in Washington and Idaho, Indoor Air. 14 (2004) 333–341. doi:10.1111/j.1600-0668.2004.00251.x.

[16] E. Simons, S.A. Hwang, E.F. Fitzgerald, C. Kielb, S. Lin, The impact of school building conditions on student absenteeism in upstate New York, Am. J. Public Health. 100 (2010) 1679–1686. doi:10.2105/AJPH.2009.165324.

[17] M.J. Mendell, E.A. Eliseeva, M.M. Davies, M. Spears, A. Lobscheid, W.J. Fisk, M.G. Apte, Association of classroom ventilation with reduced illness absence: A prospective study in California elementary schools, Indoor Air. 23 (2013) 515–528. doi:10.1111/ina.12042.

[18] J. Sundell, H. Levin, W.W. Nazaroff, W.S. Cain, W.J. Fisk, D.T. Grimsrud, F. Gyntelberg, Y.Li, A.K. Persily, A.C. Pickering, J.M. Samet, J.D. Spengler, S.T. Taylor, C.J. Weschler, Ventilation rates and health: multidisciplinary review of the scientific literature, Indoor Air. 21 (2011) 191–204.

[19] U. Haverinen-Shaughnessy, R.J. Shaughnessy, E.C. Cole, O. Toyinbo, D.J. Moschandreas, An assessment of indoor environmental quality in schools and its association with health and performance, Build. Environ. 93 (2015) 35–40. doi:10.1016/j.buildenv.2015.03.006.

[20] K. Benne, B. Griffith, N. Long, P. Torcellini, D. Crawley, T. Logee, Assessment of the Energy Impacts of Outside Air in the Commercial Sector, Golden, CO, 2009.

[21] B. Davanagere, D.I. Shirey, K. Rengarajan, F. Colacino, Mitigating the impacts of ASHRAE Standard 62 - 1989 on Florida schools., ASHRAE Trans. 103 (1997) 241–258.

[22] S.N. Rudnick, D.K. Milton, Risk of indoor airborne infection transmission

estimated from carbon dioxide concentration, Indoor Air. 13 (2003) 237–245. doi:10.1034/j.1600-0668.2003.00189.x.

[23] C.M. Liao, C.F. Chang, H.M. Liang, A probabilistic transmission dynamic model to assess indoor airborne infection risks, Risk Anal. 25 (2005) 1097–1107. doi:10.1111/j.1539-6924.2005.00663.x.

[24] G.N. Sze To, C.Y.H. Chao, Review and comparison between the Wells-Riley and dose-response approaches to risk assessment of infectious respiratory diseases, Indoor Air. 20 (2010) 2–16. doi:10.1111/j.1600-0668.2009.00621.x.

[25] J. Yan, M. Grantham, J. Pantelic, P.J. Bueno de Mesquita, B. Albert, F. Liu, S. Ehrman, D.K. Milton, Infectious virus in exhaled breath of symptomatic seasonal influenza cases from a college community, Proc. Natl. Acad. Sci. 115 (2018) 1081–1086. doi:10.1073/pnas.1716561115.

[26] W.G. Lindsley, T.A. Pearce, J.B. Hudnall, K.A. Davis, S.M. Davis, M.A. Fisher, R. Khakoo, J.E. Palmer, K.E. Clark, I. Celik, C.C. Coffey, F.M. Blachere, D.H. Beezhold, Quantity and size distribution of cough-generated aerosol particles produced by influenza patients during and after illness, J. Occup. Environ. Hyg. 9 (2012) 443–449. doi:10.1080/15459624.2012.684582.

[27] M. Nicas, W.W. Nazaroff, A. Hubbard, Toward understanding the risk of secondary airborne infection: Emission of respirable pathogens, J. Occup. Environ. Hyg. 2 (2005) 143–154. doi:10.1080/15459620590918466.

[28] A. Parham, Brent Stephens, HVAC filtration for controlling infectious airborne disease transmission in indoor environments: Predicting risk reductions and operational costs, Build. Environ. 70 (2013) 150–160. doi:10.1016/j.buildenv.2013.08.025.

[29] P. Fabian, J.J. McDevitt, W.H. DeHaan, R.O.P. Fung, B.J. Cowling, K.H. Chan, G.M. Leung, D.K. Milton, Influenza Virus in Human Exhaled Breath: An Observational Study, PLoS One. 3 (2008) e2691. doi:10.1371/journal.pone.0002691.

[30] D.K. Milton, M.P. Fabian, B.J. Cowling, M.L. Grantham, J.J. McDevitt, Influenza Virus Aerosols in Human Exhaled Breath: Particle Size, Culturability, and Effect of Surgical Masks, PLoS Pathog. 9 (2013). doi:10.1371/journal.ppat.1003205.

[31] W.G. Lindsley, F.M. Blachere, R.E. Thewlis, A. Vishnu, K.A. Davis, G. Cao, J.E. Palmer, K.E. Clark, M.A. Fisher, R. Khakoo, D.H. Beezhold, Measurements of airborne influenza virus in aerosol particles from human coughs, PLoS One. 5 (2010). doi:10.1371/journal.pone.0015100.

[32] B. Stephens, J.A. Siegel, Comparison of test methods for determining the particle removal efficiency of filters in residential and light-commercial central HVAC systems, Aerosol Sci. Technol. 46 (2012) 504–513. doi:10.1080/02786826.2011.642825.

[33] ASHRAE, Standard 52.2. Method of testing general ventilation air-cleaning devices for removal efficiency by particle size, 2012.

[34] W.J. Riley, T.E. McKone, A.C.K. Lai, W.W. Nazaroff, Indoor particulate matter of outdoor origin: Importance of size-dependent removal mechanisms, Environ. Sci. Technol. 36 (2002) 200–207. doi:10.1021/es010723y.

[35] CDC, Results for General Population Influenza Vaccination Coverage, (2018). https://www.cdc.gov/flu/fluvaxview/interactive-general-population.htm (accessed May 10, 2019).

[36] E.A. Belongia, B.A. Kieke, J.G. Donahue, R.T. Greenlee, A. Balish, A. Foust, S. Lindstrom, D.K. Shay, Effectiveness of Inactivated Influenza Vaccines Varied Substantially with Antigenic Match from the 2004–2005 Season to the 2006–2007 Season, J. Infect. Dis. 199 (2009) 159–167. doi:10.1086/595861.

[37] E.A. Belongia, B.A. Kieke, J.G. Donahue, L.A. Coleman, S.A. Irving, J.K. Meece, M. Vandermause, S. Lindstrom, P. Gargiullo, D.K. Shay, Influenza vaccine effectiveness in Wisconsin during the 2007-08 season: Comparison of interim and final results, Vaccine. 29 (2011) 6558–6563. doi:10.1016/j.vaccine.2011.07.002.

[38] M.R. Griffin, A.S. Monto, E.A. Belongia, J.J. Treanor, Q. Chen, J. Chen, H.K. Talbot, S.E. Ohmit, L.A. Coleman, G. Lofthus, J.G. Petrie, J.K. Meece, C.B. Hall, J. V. Williams, P. Gargiullo, L. Berman, D.K. Shay, Effectiveness of Non-Adjuvanted Pandemic Influenza A Vaccines for Preventing Pandemic Influenza Acute Respiratory Illness Visits in 4 U.S. Communities, PLoS One. 6 (2011) e23085. doi:10.1371/journal.pone.0023085.

[39] J.J. Treanor, H.K. Talbot, S.E. Ohmit, L.A. Coleman, M.G. Thompson, P.Y. Cheng, J.G. Petrie, G. Lofthus, J.K. Meece, J. V. Williams, L. Berman, C. Breese Hall, A.S. Monto, M.R. Griffin, E. Belongia, D.K. Shay, Effectiveness of seasonal influenza vaccines in the United States during a season with circulation of all three vaccine strains, Clin. Infect. Dis. 55 (2012) 951–959. doi:10.1093/cid/cis574.

[40] S.E. Ohmit, M.G. Thompson, J.G. Petrie, S.N. Thaker, M.L. Jackson, E.A. Belongia, R.K. Zimmerman, M. Gaglani, L. Lamerato, S.M. Spencer, L. Jackson, J.K. Meece, M.P. Nowalk, J. Song, M. Zervos, P.Y. Cheng, C.R. Rinaldo, L. Clipper, D.K. Shay, P. Piedra, A.S. Monto, Influenza vaccine effectiveness in the 2011-2012 season: Protection against each circulating virus and the effect of prior

vaccination on estimates, Clin. Infect. Dis. 58 (2014) 319–327. doi:10.1093/cid/cit736.

[41] H.Q. McLean, M.G. Thompson, M.E. Sundaram, B.A. Kieke, M. Gaglani, K. Murthy, P.A. Piedra, R.K. Zimmerman, M.P. Nowalk, J.M. Raviotta, M.L. Jackson, L. Jackson, S.E. Ohmit, J.G. Petrie, A.S. Monto, J.K. Meece, S.N. Thaker, J.R. Clippard, S.M. Spencer, A.M. Fry, E.A. Belongia, Influenza vaccine effectiveness in the United States during 2012-2013: Variable protection by age and virus type, J. Infect. Dis. 211 (2015) 1529–1540. doi:10.1093/infdis/jiu647.

[42] M. Gaglani, J. Pruszynski, K. Murthy, L. Clipper, A. Robertson, M. Reis, J.R. Chung, P.A. Piedra, V. Avadhanula, M.P. Nowalk, R.K. Zimmerman, M.L. Jackson, L.A. Jackson, J.G. Petrie, S.E. Ohmit, A.S. Monto, H.Q. McLean, E.A. Belongia, A.M. Fry, B. Flannery, Influenza Vaccine Effectiveness Against 2009 Pandemic Influenza A(H1N1) Virus Differed by Vaccine Type during 2013-2014 in the United States, J. Infect. Dis. 213 (2016) 1546–1556. doi:10.1093/infdis/jiv577.

[43] M.A. Rolfes, B. Flannery, J. Chung, A. O'Halloran, S. Garg, E.A. Belongia, M. Gaglani, R. Zimmerman, M.L. Jackson, A.S. Monto, N.B. Alden, E. Anderson, N.M. Bennett, L. Billing, S. Eckel, P.D. Kirley, R. Lynfield, M.L. Monroe, M. Spencer, N. Spina, H.K. Talbot, A. Thomas, S. Torres, K. Yousey-Hindes, J. Singleton, M. Patel, C. Reed, A.M. Fry, Effects of Influenza Vaccination in the United States during the 2017–2018 Influenza Season, Clin. Infect. Dis. (2019) 1–9. doi:10.1093/cid/ciz075.

[44] CARB, How Much Air Do We Breathe?, 1994.

[45] NCEI, Surface Data Hourly Global (DS3505), 2018.

[46] R. Wålinder, D. Norbäck, G. Wieslander, G. Smedje, C. Erwall, P. Venge, Nasal patency and biomarkers in nasal lavage–the significance of air exchange rate and type of ventilation in schools., Int Arch Occup Env. Heal. 71 (1998) 479–486.

[47] J. Wang, G. Smedje, T. Nordquist, D. Norback, Personal and demo- graphic factors and change of subjective indoor air quality reported by school children in relation to exposure at Swedish schools: a 2- year longitudinal study., Sci Total Env. 508 (2015) 288–296.

[48] U. Haverinen-Shaughnessy, D. Moschandreas, R. Shaughnessy, Association between substandard classroom ventilation rates and students' academic achievement, Indoor Air. 21 (2011) 121–131. doi:10.1111/j.1600-0668.2010.00686.x.

[49] U.S.E.I. Administration, Table 5.6.A. Average Price of Electricity to Ultimate Customers by End-Use Sector, (2019). https://www.eia.gov/electricity/monthly/epm_table_grapher.php?t=epmt_5_6_a (accessed May 10, 2019).

[50] New Hampshire Department of Health and Human Services. NH School Absenteeism Reporting, (2019). https://www.dhhs.nh.gov/dphs/cdcs/influenza/schoolsurveillance.htm (accessed May 10, 2019).

[51] New Jersey Department of Health Services, Communicable Disease Service: Influenza-like Illness Weekly Reports, (2019). https://www.nj.gov/health/cd/statistics/flu-stats/ (accessed May 10, 2019).

[52] J.J. Mcdevitt, P. Koutrakis, S.T. Ferguson, J.M. Wolfson, M. Patricia, M. Martins, J. Pantelic, D.K. Milton, Development and Performance Evaluation of an Exhaled-Breath Bioaerosol Collector for Influenza Virus, Aerosol Sci Technol. 47 (2013) 444–451. doi:10.1080/02786826.2012.762973.Development.

[53] G.J. Harper, Airborne micro-organisms: survival tests with four viruses, J. Hyg. (Lond). 59 (1961) 479–486. https://www.ncbi.nlm.nih.gov/pubmed/13904777.

[54] J.H. Hemmes, K.C. Winkler, Kool, S M, Virus Survival as a Seasonal Factor in Influenza and Poliomyelitis, Nature. 188 (1960) 430–431. doi:10.1038/188430a0.

[55] W. Yang, L.C. Marr, Dynamics of Airborne influenza A viruses indoors and dependence on humidity, PLoS One. 6 (2011). doi:10.1371/journal.pone.0021481.

[56] C.J. Noakes, P. Andrew Sleigh, Mathematical models for assessing the role of airflow on the risk of airborne infection in hospital wards, J. R. Soc. Interface. 6 (2009). doi:10.1098/rsif.2009.0305.focus.

[57] National Center for Educational Statistics, Education Expenditures by Country, (2018). https://nces.ed.gov/programs/coe/indicator_cmd.asp (accessed May 10, 2019).

[58] L. Lesnick, R.L. Corsi, A. Novoselac, Ventilation and Corresponding CO2 Levels in High School Classrooms, in: Present. 2017 Annu. ASHRAE Conf. Long Beach, CA, June 24-28, 2017., n.d.